Preprints of the 19th World Congress
The International Federation of Automatic Control
Cape Town, South Africa. August 24-29, 2014

Distributed MPC for Frequency Regulation in Multi-Terminal HVDC Grids ⋆

Paul Mc Namara *, **Ronan Meere** **, **Terence O'Donnell** **, **Seán McLoone** ***

* *Dynamics and Control Research Group, Dept. Electronic Engineering, Callan Building, NUI Maynooth, Maynooth, Kildare, Ireland (e-mail: pmcnamara@eeng.nuim.ie).*
** *Electricity Research Centre, Engineering & Materials Science Centre, University College Dublin, Belfield, Dublin 4, Ireland.*
*** *Energy, Power and Intelligent Control Research Cluster, School of Electronics, Electrical Engineering and Computer Science, Queen's University Belfast, Belfast, Northern Ireland.*

Abstract: High Voltage Direct Current (HVDC) lines allow large quantities of power to be transferred between two points in an electrical power system. A Multi-Terminal HVDC (MTDC) grid consists of a meshed network of HVDC lines, and this allows energy reserves to be shared between a number of AC areas in an efficient manner. Secondary Frequency Control (SFC) algorithms return the frequencies in areas connected by AC or DC lines to their original setpoints after Primary Frequency Controllers have been called following a contingency. Where multiple TSOs are responsible for different parts of a MTDC grid it may not be possible to implement SFC from a centralised location. Thus, in this paper a simple gain based distributed Model Predictive Control strategy is proposed for Secondary Frequency Control of MTDC grids which allows TSOs to cooperatively perform SFC without the need for centralised coordination.

Keywords: Multi-terminal HVDC; Distributed MPC; Secondary Frequency Control.

1. INTRODUCTION

In line with the framework outlined in the 20-20-20 EU initiative (EWEA, 2009), the future common European electricity market will evolve so as to cater for the projected high volume of intermittent renewable energy resources expected across the European grid. The sharing of these stochastic renewable energy sources over large areas will also have the effect of mitigating some of the issues associated with having large penetrations of renewables in the generation mix. The development of a European interconnected grid or "Supergrid" has received widespread attention as a means of achieving this goal. This will facilitate access to variable renewable sources, such as wind from the North of Europe and solar from the South of Europe and North Africa, which then can be aggregated across the entire European grid allowing higher penetrations of low carbon energy overall without threatening the stability of the system (Van Hertem and Ghandhari, 2010).

High Voltage Direct Current (HVDC) transmission facilitates the transfer of large quantities of electrical power over long distances by utilising DC power transmission (Kundur, 1994). Most HVDC lines are point-to-point lines that transfer energy between only two AC areas, with a converter on each side. Modern Voltage Source Converter (VSC) based HVDC technologies allow a number of HVDC lines to be connected to a single DC grid terminal (de Courreges d'Ustou, 2012). Thus Multi-Terminal HVDC (MTDC) grids can be constructed, which consist of a meshed HVDC grid with a number of connections to AC grids. Consequently this facilitates the sharing of energy reserves over large areas for the purposes of enhancing stability in an efficient manner across the various AC areas. Thus there has been much interest in developing coordinated control methods which allow power injections to and from the DC grid to support frequency in connected AC areas.

A number of Primary Frequency Control (PFC) algorithms, which operate on the milliseconds to seconds scale, have been proposed for sharing primary reserves over MTDC grids. Several of these have involved using direct communication between areas (Dai et al., 2010; Chaudhuri and Chaudhuri, 2013; Machowski et al., 2013). However, these algorithms can be non-robust to communication delays or failures, as shown in Dai et al. (2010), and hence a number of methods that do not rely on communication between areas have been proposed. These operate by manipulating the DC voltages on the grid in a decentralised fashion in order to regulate the power flows into or out of AC areas and the MTDC grid (Dai et al., 2012; Silva et al., 2012; Chaudhuri et al., 2013; Egea-Alvarez et al., 2013). As is the case with decentralised PFC in AC areas, it is necessary to provide Secondary Frequency Control (SFC), which acts on the seconds to minutes scale, so as

⋆ This research was funded by Science Foundation Ireland as part of the Sustainable Electrical Energy Systems (SEES) Cluster (grant 09/SRC/E1780).

Copyright © 2014 IFAC

to satisfy long-term frequency regulation goals across areas connected to MTDC grids.

A decentralised PI-based SFC strategy was proposed in Dai (2011), and a PID-based extension of this method was optimised centrally in de Courreges d'Ustou (2012). In de Courreges d'Ustou (2012) it is shown that by optimising the controller gains the performance of the system can be significantly improved. However, there is an underlying assumption here that it is possible to optimise these controller parameters from a central location with access to the state-space of the entire grid. Transmission System Operators (TSOs) are responsible for the balancing of the electricity supply to match demand across power grids. Different sections of large power systems, such as the European grid, are controlled by separate TSOs. As it is the responsibility of these TSOs to ensure stable power system control in the areas under their jurisdiction, it is unlikely that they would be willing to give authority to a third party to determine their controller gains. Also, it would be necessary for legal frameworks to be in place such that different TSOs' state-space information could be made available to the centralised coordinator. Distributed optimal control solutions can circumvent these issues by allowing TSOs to remain autonomous, while remaining capable of coordinating their actions with other TSOs via a negotiation process.

Model Predictive Control (MPC) (Maciejowski, 2002) algorithms enable the optimal control of a system based on the use of state-space predictions, and in recent years, there has been extensive research in the field of distributed MPC. Here a number of controllers, called control agents, are responsible for the control of separate interconnected subsystems in a system, and through inter-agent communication, it is possible for them to collectively achieve performance that approximates that of a centralised MPC controller (Christofides et al., 2013).

In this paper, it is demonstrated how a simple gain based distributed MPC controller can be used for SFC over a MTDC grid. It will be seen that through inter-area communication it is possible for the controllers to achieve similar performance to that of a centralised MPC for SFC, without the need for centralised coordination. Thus the issues outlined previously with regard to centralised coordination of TSOs for SFC could be could be circumvented.

The remainder of the paper is structured as follows. In Section 2, modelling and decentralised PFC of a MTDC system are described. Then Sections 3 and 4 introduce centralised and distributed MPC, respectively. Section 5, derives the state-space model needed for the centralised and distributed MPC implementations. Simulations and results are presented in Section 6, and conclusions and future work are discussed in Section 7.

2. MODELLING AND FREQUENCY CONTROL FOR MULTI-TERMINAL HVDC GRIDS

2.1 Modelling

A MTDC grid is composed of a DC grid and N AC areas, each with a converter which serves as an interface for transferring power to and from the DC grid, as in Fig. 1

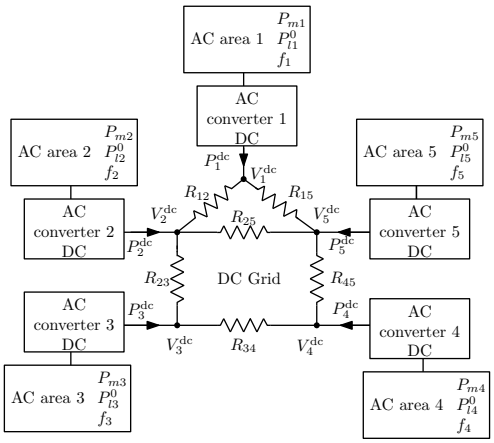

Fig. 1. A multi-terminal DC grid connecting $N = 5$ AC areas via converters (Sarlette et al., 2012).

(Sarlette et al., 2012). Each AC area i, for $i = 1, 2, \ldots, N$, has a state vector $(f_i, P_{\mathrm{m}i}) \in \Re^2$, and is governed by the following dynamic equations:

$$J_i \frac{\mathrm{d}}{\mathrm{d}t} f_i(t) = \frac{P_{\mathrm{m}i}(t) - P_{\mathrm{l}i}(t) - P_i^{\mathrm{dc}}(t)}{4\pi^2 f_i(t)} - D_{\mathrm{g}i}(f_i(t) - \bar{f}_i), \quad (1)$$

$$\tau_i \frac{\mathrm{d}}{\mathrm{d}t} P_{\mathrm{m}i}(t) = P_{\mathrm{m}i}^0(t) - P_{\mathrm{m}i}(t) - \frac{P_{\mathrm{nom},i}}{\sigma_i} \frac{f_i(t) - \bar{f}_i}{\bar{f}_i}, \quad (2)$$

$$P_{\mathrm{l}i}(t) = P_{\mathrm{l}i}^0(t)(1 + D_{\mathrm{l}i}(f_i(t) - \bar{f}_i)), \quad (3)$$

where J_i is the moment of inertia of aggregated area i (kg m^2), $f_i(t)$ is the frequency (Hz), $P_{\mathrm{m}i}(t)$ is the mechanical power (W), $P_{\mathrm{l}i}(t)$ is the load disturbance considering frequency effects (W), $P_i^{\mathrm{dc}}(t)$ is the DC power AC area i is injecting into the DC grid (W), $D_{\mathrm{g}i}$ is the damping factor (W s^2), $\bar{f}_i$ is the nominal frequency (Hz), τ_i is the time constant for power adjustment (s), $P_{\mathrm{m}i}^0(t)$ is the reference mechanical power which is manipulated using SFC (W), σ_i is the generator droop (dimensionless), $P_{\mathrm{l}i}^0(t)$ is the nominal load disturbance at bus i (W), and $D_{\mathrm{l}i}$ is the sensitivity of $P_{\mathrm{l}i}(t)$ to deviations of the frequency from the nominal frequency (s) (Kundur, 1994).

The dynamics of the HVDC converters are not significant at the time scales considered in this work and so it is assumed that these values are taken at their steady state values. The power injected into the HVDC grid is equal to that leaving the grid, i.e.,

$$P_1^{\mathrm{dc}}(t) + \ldots + P_N^{\mathrm{dc}}(t) = 0. \quad (4)$$

A negative $P_i^{\mathrm{dc}}(t)$ indicates area i is receiving P_i^{dc} W from the HVDC grid, and a positive $P_i^{\mathrm{dc}}(t)$ indicates area i is injecting P_i^{dc} W into the HVDC grid. Denoting $V_i^{\mathrm{dc}}(t)$ as the DC voltage of area i, it follows that,

$$P_i^{\mathrm{dc}}(t) = \sum_{j=1}^{N} \frac{V_i^{\mathrm{dc}}(t)(V_i^{\mathrm{dc}}(t) - V_j^{\mathrm{dc}}(t))}{R_{ij}}, \quad (5)$$

where $R_{ij} = R_{ji}$ is the resistance in the HVDC line connecting areas i and j, and $R_{ij} = \infty$ if areas i and j are not connected by a DC line.

2.2 Primary Frequency Control

A communication-free decentralised PFC law was proposed for the sharing of primary reserves amongst AC

areas over the HVDC network in Sarlette et al. (2012). This is given as follows

$$v_i = \gamma_i x_{\mathrm{f}i}, \tag{6}$$

where the DC input voltage deviation at area i, $v_i(t) = V_i^{\mathrm{dc}}(t) - \bar{V}_i^{\mathrm{dc}}$, where $\bar{V}_i^{\mathrm{dc}}$ is the operating point of V_i^{dc} at equilibrium, the state $x_{\mathrm{f}i}$ is given by $x_{\mathrm{f}i} = f_i(t) - \bar{f}_i$, and γ_i is agent i's DC voltage PFC gain. This control law effectively shares resources amongst AC areas and the conditions for stable control under this law are given in (Sarlette et al., 2012). While this PFC acts on the milliseconds to seconds time scale to counteract disturbances in the AC areas, it does not return the AC areas to their original setpoints, and hence a secondary level controller is needed to manipulate $P_{\mathrm{m}i}^0(t)$ over longer time scales (typically seconds to minutes) in order to achieve this objective.

2.3 Secondary Frequency Control

The objective of SFC in area i is to maintain the frequency and net interchange power with connected areas at their scheduled values, $\bar{f}_i$ and $\bar{P}_i^{\mathrm{dc}}$, respectively. Assuming a discrete-time controller for SFC, at sample step k SFC seeks to minimise the following objective function for area i, $\Psi_i(k)$, defined here as

$$\Psi_i(k) = Q_{\mathrm{f}i} x_{\mathrm{f}i}^2(k+1) + Q_{\mathrm{z}i} z_i^2(k+1), \tag{7}$$

where $z_i = P_i^{\mathrm{dc}}(t) - \bar{P}_i^{\mathrm{dc}}$, and $Q_{\mathrm{f}i}$ and $Q_{\mathrm{z}i}$ are weights which determine the relative importance of minimising $x_{\mathrm{f}i}(k)$ and $z_i(k)$, respectively. In the following sections centralised and distributed MPC will be introduced and it will then be shown how SFC can be achieved using a MPC framework.

3. MODEL PREDICTIVE CONTROL

Model Predictive Control is an optimisation based control technique that uses state-space based predictions in order to form optimal inputs to a system over a prediction horizon. While inputs are calculated over the full prediction horizon, only the input for the first sample step of the prediction horizon is applied to the system, and this process is repeated every sample step.

A discrete-time, linear, time-invariant state-space model is given as follows,

$$\boldsymbol{x}(k+1) = \boldsymbol{A}\boldsymbol{x}(k) + \boldsymbol{B}\boldsymbol{u}(k) \tag{8}$$

$$\boldsymbol{y}(k) = \boldsymbol{C}\boldsymbol{x}(k), \tag{9}$$

where $\boldsymbol{x}(k)$ is the state, $\boldsymbol{u}(k)$ are the inputs, and $\boldsymbol{y}(k)$ are the outputs of the systems at a sample time k. Matrices $\boldsymbol{A}$, $\boldsymbol{B}$, and $\boldsymbol{C}$ are the relevant state-space matrices. An incremental state-space model is used for control in order to ensure integral action:

$$\boldsymbol{x}^{\mathrm{aug}}(k+1) = \hat{\boldsymbol{A}}\boldsymbol{x}^{\mathrm{aug}}(k) + \hat{\boldsymbol{B}}\Delta\boldsymbol{u}(k) \tag{10}$$

$$\boldsymbol{y}(k+1) = \hat{\boldsymbol{C}}\boldsymbol{x}^{\mathrm{aug}}(k+1), \tag{11}$$

where $\boldsymbol{x}^{\mathrm{aug}}(k) = [\Delta\boldsymbol{x}^{\mathrm{T}}(k)\ \boldsymbol{x}^{\mathrm{T}}(k)]^{\mathrm{T}}$ is the augmented state vector, $\Delta\boldsymbol{z}(k) = \boldsymbol{z}(k) - \boldsymbol{z}(k-1)$ denotes the increment in $\boldsymbol{z}$ between samples k and $k-1$, and $\hat{\boldsymbol{A}}$, $\hat{\boldsymbol{B}}$, $\hat{\boldsymbol{V}}$, and $\hat{\boldsymbol{C}}$ are the incremental state-space matrices.

To simplify notation, the prediction vector, over a horizon H is first introduced. For a general vector $\boldsymbol{p}$, its prediction vector is $\tilde{\boldsymbol{p}}(k) = [\boldsymbol{p}^{\mathrm{T}}(k) \dots \boldsymbol{p}^{\mathrm{T}}(k+H-1)]^{\mathrm{T}}$. State and output predictions for the system over the prediction horizon are then determined using (10) and (11) as follows:

$$\tilde{\boldsymbol{x}}^{\mathrm{aug}}(k+1) = \hat{\boldsymbol{A}}^{\mathrm{f}}\boldsymbol{x}^{\mathrm{aug}}(k) + \hat{\boldsymbol{B}}^{\mathrm{f}}\Delta\tilde{\boldsymbol{u}}(k) \tag{12}$$

$$\tilde{\boldsymbol{y}}^{\mathrm{aug}}(k) = \hat{\boldsymbol{C}}^{\mathrm{f}}\tilde{\boldsymbol{x}}^{\mathrm{aug}}(k), \tag{13}$$

where $\hat{\boldsymbol{A}}^{\mathrm{f}}$, $\hat{\boldsymbol{B}}^{\mathrm{f}}$, and $\hat{\boldsymbol{C}}^{\mathrm{f}}$ are the state-space prediction matrices. The derivation of these matrices is based on iteratively solving for $\boldsymbol{x}(k+a+1)$ based on $\boldsymbol{x}(k+a)$ using (8) and is well established in the literature (Maciejowski, 2002).

MPC problems are constructed to fulfill control objectives for a system based on knowledge of $\boldsymbol{x}(k)$. A cost function, $J(\boldsymbol{x}^{\mathrm{aug}}(k), \Delta\tilde{\boldsymbol{u}}(k))$ (which will henceforth be denoted by $J(k)$), is designed so as to embody the system's objectives. Typically this cost function is quadratic in $\Delta\tilde{\boldsymbol{u}}$ and is expressed as:

$$\begin{aligned} J(k) &= \tilde{\boldsymbol{e}}^{\mathrm{T}}(k+1)\boldsymbol{Q}\tilde{\boldsymbol{e}}(k+1) + \Delta\tilde{\boldsymbol{u}}^{\mathrm{T}}(k)\boldsymbol{R}\Delta\tilde{\boldsymbol{u}}(k) \\ &= \Delta\tilde{\boldsymbol{u}}^{\mathrm{T}}(k)\boldsymbol{H}\Delta\tilde{\boldsymbol{u}}(k) + \Delta\tilde{\boldsymbol{u}}^{\mathrm{T}}(k)\boldsymbol{f} + \mu \end{aligned} \tag{14}$$

where the error vector, $\boldsymbol{e}(k+1) = \boldsymbol{y}(k+1) - \boldsymbol{r}(k+1)$, $\boldsymbol{r}(k)$ is a vector of the setpoints at sample step k, $\boldsymbol{Q}$ and $\boldsymbol{R}$ are weighting matrices, $\boldsymbol{H}$ is a square symmetric non-singular matrix, $\boldsymbol{f}$ is a vector, and μ is a constant which does not depend on $\Delta\tilde{\boldsymbol{u}}(k)$. For the unconstrained case, an analytical solution for the inputs can then be found by finding the value of $\Delta\tilde{\boldsymbol{u}}(k)$ that minimises $J(k)$.

The optimal choice of controls $\Delta\tilde{\boldsymbol{u}}^*(k)$ is obtained when,

$$\frac{\partial}{\partial\Delta\tilde{\boldsymbol{u}}(k)} J(k) = 2\boldsymbol{H}\Delta\tilde{\boldsymbol{u}}(k) + \boldsymbol{f} = 0, \tag{15}$$

where a superscripted * denotes the optimum value of a variable. This yields the solution,

$$\Delta\tilde{\boldsymbol{u}}^*(k) = -\frac{1}{2}\boldsymbol{H}^{-1}\boldsymbol{f}. \tag{16}$$

The input at the start of the horizon $\boldsymbol{u}(k)$ is applied to the system and this process is repeated each sample step. Unconstrained MPC in this form is equivalent in performance to a Finite Horizon Linear Quadratic Regulator.

In the above formulation MPC is carried out from a central location. At each sample step each area must send the central controller state measurements, and the controller must have access to the full state-space of each of the areas to formulate the control problem. Having calculated the input vector the central controller then sends the inputs to each area. This may be impractical in the case where a MTDC grid connects a number of areas under the control of different TSOs, as TSOs may be reluctant to share internal state-space information due to privacy concerns. The need for long distance communication between the controller and connected areas could also induce delays, and the system would not be robust to the failure of the central control agent. In the following section distributed MPC is described where control agents responsible for interconnected subsystems can communicate with each other in order to coordinate their responses, thus avoiding the need for a central coordinator.

4. DISTRIBUTED MPC

Consider a system consisting of n non-overlapping subsystems. A discrete-time, linear, time-invariant state-space model is used to model the dynamics of each subsystem,

$$\boldsymbol{x}_a(k+1) = \boldsymbol{A}_a\boldsymbol{x}_a(k) + \boldsymbol{B}_a\boldsymbol{u}_a(k) + \boldsymbol{V}_a\boldsymbol{v}_a(k) \quad (17)$$

$$\boldsymbol{y}_a(k) = \boldsymbol{C}_a\boldsymbol{x}_a(k), \quad (18)$$

where $\boldsymbol{x}_a(k)$ is the state of subsystem a, $\boldsymbol{u}_a(k)$ are subsystem inputs, $\boldsymbol{y}_a(k)$ are subsystem outputs, and $\boldsymbol{v}_a(k)$ are external inputs from other subsystems that influence subsystem a at sample step k. The matrices $\boldsymbol{A}_a$, $\boldsymbol{B}_a$, $\boldsymbol{V}_a$, and $\boldsymbol{C}_a$ are the relevant state-space matrices. The incremental state-space model is given by:

$$\boldsymbol{x}_a^{\mathrm{aug}}(k+1) = \hat{\boldsymbol{A}}_a\boldsymbol{x}_a^{\mathrm{aug}}(k) + \hat{\boldsymbol{B}}_a\Delta\boldsymbol{u}_a(k) + \hat{\boldsymbol{V}}_a\Delta\boldsymbol{v}_a(k) \quad (19)$$

$$\boldsymbol{y}_a(k+1) = \hat{\boldsymbol{C}}_a\boldsymbol{x}_a^{\mathrm{aug}}(k+1), \quad (20)$$

where $\boldsymbol{x}_a^{\mathrm{aug}}(k) = [\Delta\boldsymbol{x}_a^{\mathrm{T}}(k)\ \boldsymbol{x}_a^{\mathrm{T}}(k)]^{\mathrm{T}}$ is the augmented state vector of the a^{th} subsystem and $\hat{\boldsymbol{A}}_a$, $\hat{\boldsymbol{B}}_a$, $\hat{\boldsymbol{V}}_a$, and $\hat{\boldsymbol{C}}_a$ are the incremental state-space matrices for subsystem a. State and output predictions for subsystem a are performed in the same way as in the centralised case with predictive matrices $\hat{\boldsymbol{A}}_a^{\mathrm{f}}$, $\hat{\boldsymbol{B}}_a^{\mathrm{f}}$, $\hat{\boldsymbol{V}}_a^{\mathrm{f}}$, and $\hat{\boldsymbol{C}}^{\mathrm{f}}$.

The Non-Cooperative distributed MPC (NCdMPC) is now described. Further details on the derivation of this algorithm are given in (Negenborn et al., 2008). Let agent $j \in \mathcal{N}_a$ be connected to agent a, where $\mathcal{N}_a$ is the set of agents connected to agent a by a common variable. The interconnecting input vector, $\boldsymbol{w}_{ja}^{\mathrm{in}}$, is defined as the vector of inputs to control problem a from agent $j \in \mathcal{N}_a^{\mathrm{in}}$, where $\mathcal{N}_a^{\mathrm{in}} \subseteq \mathcal{N}_a$ is the ordered set of agents connected to agent a by an interconnecting input. Likewise, the interconnecting output vector $\boldsymbol{w}_{ja}^{\mathrm{out}}$ is defined as the vector of outputs to control problem $j \in \mathcal{N}_a^{\mathrm{out}}$ from agent a, where $\mathcal{N}_a^{\mathrm{out}} \subseteq \mathcal{N}_a$ is the ordered set of agents connected to agent a by an interconnecting output.

At each sample step k, a so called NCdMPC cycle is carried out. This NCdMPC cycle is a process that consists of a number of iterations in which agents optimise in a serial fashion. The optimisation problem of agent a, for iteration l of the distributed MPC cycle, at sample step k is:

$$\boldsymbol{\theta}_a^*(k,l) = \arg\min_{\boldsymbol{\theta}_a(k,l)} \left(J_a^{\mathrm{local}}(k,l) + J_a^{\mathrm{inter}}(k,l) \right), \quad (21)$$

where $\boldsymbol{\theta}_a(k,l) = [\Delta\tilde{\boldsymbol{u}}_a^{\mathrm{T}}(k,l), \Delta\tilde{\boldsymbol{w}}_a^{\mathrm{inT}}(k,l)]^{\mathrm{T}}$.

Here $J_a^{\mathrm{local}}(k,l)$ represents the local control goals, and as in the centralised case, is usually a quadratic function of $\boldsymbol{\theta}_a^*(k,l)$. The function is usually chosen so as to minimise the difference between some system outputs and their corresponding setpoints, and this will often be balanced against the controller effort needed to achieve these goals.

The interconnecting cost for agent a, $J_a^{\mathrm{inter}}(k,l)$, is given by:

$$J_a^{\mathrm{inter}}(k,l) = \sum_{j\in\mathcal{N}_a} J_{ja}^{\mathrm{inter}}(k,l), \quad (22)$$

and $J_{ja}^{\mathrm{inter}}(k,l)$ is the cost associated with the inter-agent coordination with agent j given by:

$$J_{ja}^{\mathrm{inter}}(k,l) = \begin{bmatrix} \tilde{\boldsymbol{\lambda}}_{ja}^{\mathrm{in}}(k,l) \\ -\tilde{\boldsymbol{\lambda}}_{aj}^{\mathrm{in}}(k,l) \end{bmatrix}^{\mathrm{T}} \begin{bmatrix} \tilde{\boldsymbol{w}}_{ja}^{\mathrm{in}}(k,l) \\ \tilde{\boldsymbol{w}}_{ja}^{\mathrm{out}}(k,l) \end{bmatrix} + \frac{c}{2} \left\| \begin{bmatrix} \tilde{\boldsymbol{w}}_{ja}^{\mathrm{in}}(k,l) - \tilde{\boldsymbol{w}}_{aj,\mathrm{prev}}^{\mathrm{out}}(k,l) \\ \tilde{\boldsymbol{w}}_{ja}^{\mathrm{out}}(k,l) - \tilde{\boldsymbol{w}}_{aj,\mathrm{prev}}^{\mathrm{in}}(k,l) \end{bmatrix} \right\|_2^2, \quad (23)$$

where $\tilde{\boldsymbol{\lambda}}_{ja}^{\mathrm{in}}(k,l)$ is the vector of Lagrange multipliers associated with the equality constraint $\tilde{\boldsymbol{w}}_{ja}^{\mathrm{in}}(k) = \tilde{\boldsymbol{w}}_{aj}^{\mathrm{out}}(k)$, c is a positive constant, and $\tilde{\boldsymbol{w}}_{aj,\mathrm{prev}}^{\mathrm{out}}(k,l)$ and $\tilde{\boldsymbol{w}}_{aj,\mathrm{prev}}^{\mathrm{in}}(k,l)$ are taken as the most recently updated values of $\tilde{\boldsymbol{w}}_{aj}^{\mathrm{out}}(k,l)$ and $\tilde{\boldsymbol{w}}_{aj}^{\mathrm{in}}(k,l)$, respectively.

When $J_a^{\mathrm{local}}(k,l)$ is quadratic in $\boldsymbol{\theta}_a^*(k,l)$ it is then possible to express (21) as follows:

$$\boldsymbol{\theta}_a^*(k,l) = \arg\min_{\boldsymbol{\theta}_a(k,l)} \boldsymbol{\theta}_a^{\mathrm{T}}(k,l)\boldsymbol{H}_a\boldsymbol{\theta}_a(k,l) + \boldsymbol{\theta}_a^{\mathrm{T}}(k,l)\boldsymbol{f}_a + \mu_a, \quad (24)$$

where $\boldsymbol{H}_a$ is a square symmetric matrix, $\boldsymbol{f}_a$ is a vector, and μ_a is a constant which does not depend on $\boldsymbol{\theta}_a(k,l)$. When no inequality constraints are considered, an analytical solution for $\boldsymbol{\theta}_a^*(k,l)$ can then be found, using the same logic as in (15) and (16). This allows the NCdMPC algorithm to be implemented using a simple constant gain matrix.

Each agent solves (24) in a serial fashion, and after the agents have optimised, they send updated values of interconnecting variables to their neighbours. Agents who are not connected by an interconnecting variable may optimise in parallel too. When each agent has performed one optimisation during iteration l of the distributed MPC cycle, the Lagrange multipliers are updated as follows for iteration $l+1$:

$$\tilde{\boldsymbol{\lambda}}_{ja}^{\mathrm{in}}(k,l+1) = \tilde{\boldsymbol{\lambda}}_{ja}^{\mathrm{in}}(k,l) + c\left(\tilde{\boldsymbol{w}}_{ja}^{\mathrm{in}}(k,l) - \tilde{\boldsymbol{w}}_{aj}^{\mathrm{out}}(k,l)\right). \quad (25)$$

The distributed MPC iterations terminate when:

$$||\tilde{\boldsymbol{\lambda}}_{ja}^{\mathrm{in}}(k,l+1) - \tilde{\boldsymbol{\lambda}}_{ja}^{\mathrm{in}}(k,l)||_\infty \leq \epsilon, \forall j \in \mathcal{N}_a, \forall a = \{1,\ldots,n\}, \quad (26)$$

where ϵ is a small tolerance and $\|.\|_\infty$ denotes the infinity norm. Upon convergence agents apply $\boldsymbol{u}_a(k)$, for $a = 1,\ldots,n$ to the system, and the NCdMPC process is then repeated each time step. In certain cases, there may be constraints on the number of NCdMPC iterations allowed in a sample step. In these cases, the NCdMPC iterations can be terminated prematurely and the inputs which have been calculated by each agent in the most recent iteration can be applied to the system. While this can result in sub-optimal performance, stable control performance is usually maintained in such cases.

5. SECONDARY FREQUENCY CONTROL USING MPC IN MTDC SYSTEMS

In order to develop a linear cost function to implement MPC for SFC, it is necessary to linearise equations (1) and (5), in order to generate state predictions. These linearisations are given as follows, as in (Dai, 2011):

$$\frac{\mathrm{d}}{\mathrm{d}t}f_i(t) = \frac{P_{\mathrm{m}i}(t) - P_{\mathrm{l}i}(t) - P_i^{\mathrm{dc}}(t)}{4\pi^2\bar{f}_i J_i} - \frac{D_{\mathrm{g}i}}{J_i}(f_i(t) - \bar{f}_i), \quad (27)$$

$$z_i = \sum_{j=1}^{N} \frac{\bar{V}_i^{\mathrm{dc}}(v_i - v_j)}{R_{ij}} = \sum_{j=1}^{N} \frac{\bar{V}_i^{\mathrm{dc}}(\gamma_i x_{\mathrm{f}i} - \gamma_j x_{1j})}{R_{ij}}, \quad (28)$$

where $z_i = P_i^{\mathrm{dc}}(t) - \bar{P}_i^{\mathrm{dc}}$, where $\bar{P}_i^{\mathrm{dc}}$ is the operating point for the DC power in area i. It is assumed in (28) that each area is under the PFC law given in (6).

State space equations can be used for predictions by linearising equations (2) and (27) about an operating

point, with the state of agent i given by $\boldsymbol{x}_i = [x_{\mathrm{f}i}, x_{\mathrm{P}i}]^{\mathrm{T}}$, where $x_{\mathrm{P}i} = P_{\mathrm{m}i}(t) - \bar{P}_{\mathrm{m}i}$, and $\bar{P}_{\mathrm{m}i}$ is the operating point for $P_{\mathrm{m}i}(t)$. The linearised input of agent i is given by $u_i = P^0_{\mathrm{m}i}(t) - \bar{P}^0_{\mathrm{m}i}$, where $\bar{P}^0_{\mathrm{m}i}$ is the operating point for $P^0_{\mathrm{m}i}(t)$, and the linearised output by $y_i = \boldsymbol{C}_i \boldsymbol{x}_i$, where $\boldsymbol{C}_i = [1, 0]$. Each AC area a connected to the MTDC grid, for $a = 1, \ldots, N$, has an associated local cost function J_a^{local}. Using state-space predictions each agent's local cost function is given by:

$$J_a^{\mathrm{local}} = \sum_{p=k+1}^{k+H} \left(\Psi_a(p) + R_a \Delta u_a^2(p) \right). \tag{29}$$

This cost function is designed to balance the minimisation of $\Psi_a(p)$ against the predicted control effort needed to achieve this at each sample step over the prediction horizon. This cost function can be formulated depending on the particular MPC algorithm being implemented.

6. SIMULATIONS

Simulations were carried out on a testbed to evaluate the performance of four different MPC based SFC implementations using Matlab and Simulink. The first two implementations were a centralised MPC (CMPC) and a NCdMPC with $c = 1$ and tolerance $\epsilon = 1{\times}10^{-3}$, which was allowed to fully converge at each sample step. The third was an NCdMPC which terminated after only 1 iteration at each sample step (denoted NCdMPC1). The final was a decentralised MPC (deMPC) algorithm, where agents did not exchange information, basing their control only on local information. For the purposes of minimisation of ΔP_j^{dc} in the decentralised case, agent j assumed that the DC voltages at HVDC connected areas were constant and maintained their initial values for the duration of the simulation.

The testbed for simulations was the 5-agent testbed given in Fig. 1. The parameter values for the AC and DC grids are given in Table 1. The system was simulated for 40 s, and at time $t = 0$, $P^0_{\mathrm{l}1}$ was increased by 5% of its original value which necessitated responses from the primary and secondary frequency controllers. The system was simulated in discrete time with a sample step of 0.01 s using nonlinear dynamics equations (1), (2), (3), and (5).

A sample step of 0.5s was used for control and the state space, based on (27) and (28), was discretised accordingly. The prediction horizon was chosen as $H = 10$. Disturbances d_i were not known a priori or measurable for the purposes of control. The weights for the MPC algorithms were given as follows: $Q_{\mathrm{f}a} = 1$, $Q_{\mathrm{z}a} = 0.01$, and $R_a = 0.1$, for $a = 1, \ldots, 5$. Warm starts were used for the Lagrange multipliers in the NCdMPC cases, where the optimal values of Lagrange multipliers from sample step $k-1$ were used to initialise the Lagrange multipliers at the next sample step k. Agents that do not share an interconnecting variable can perform their optimisations in parallel, for the NCdMPC cases. Therefore, in each NCdMPC cycle the first agents to optimise in parallel were agents 1 and 4, then agents 3 and 5 optimised in parallel, and finally agent 2.

AC grid parameters					
Area	1	2	3	4	5
f_{nom} (Hz)	50	50	50	50	50
P^0_{m} (MW)	50	80	50	30	80
P_{nom} (MW)	50	80	50	30	80
J (kg m^2)	2026	6485	6078	2432	4863
D_g (W s^2)	48.4	146.3	140	54.9	95.1
T_{sm} (s)	1.5	2.0	2.5	2	1.8
P^0_{l} (MW)	100.42	59.58	40.31	49.70	39.59
D_l (Hz^{-1})	0.01	0.01	0.01	0.01	0.01
$\bar{V}^{\mathrm{dc}}$ (kV)	99.17	99.6	99.73	99.59	100
$\bar{P}^{\mathrm{dc}}$ (MW)	-50.4	20	10	-20	40.4
σ (no units)	0.02	0.04	0.06	0.04	0.03
γ (kV Hz^{-1})	1	1	1	1	1
τ (s)	1.5	2	2.5	2	1.8
DC grid resistances (Ω)					
R_{12}	R_{15}	R_{23}	R_{25}	R_{34}	R_{45}
1.39	4.17	2.78	6.95	2.78	2.78

Table 1. AC and DC grid parameters.

MPC	CMPC	NCdMPC	NCdMPC1	deMPC
$J_{\mathrm{sim}}(\times 10^{-6})$	138	194.9	191.3	635

Table 2. J_{sim} for each MPC control scheme.

6.1 Results

The plots of f_1 and P_1^{dc} under deMPC, CMPC, NCdMPC, and NCdMPC1, are given in Fig. 2 and Fig. 3, respectively. The following performance criterion was used in Table 2 to evaluate the performance of each of the controllers over the course of the entire simulation:

$$J_{\mathrm{sim}} = \sum_{a=1}^{5} \sum_{p=0}^{k_f} \left(\Psi_a(p) + R_a \Delta u_a^2(p) \right). \tag{30}$$

where k_f is the total number of control samples during the simulation.

The following can be observed from both the simulations and values of J_{sim}. The CMPC gives the best J_{sim} performance and provides shortest settling time, in terms of both the damped response and settling times. The deMPC case gives the worst J_{sim} performances, provides a highly underdamped response, and has the longest settling time. Both NCdMPC and NCdMPC1 provide similar responses with damping and settling times comparable to that of CMPC. The maximum number of NCdMPC iterations needed to achieve this performance in a given sample step is 2, as shown in Fig. 4.

Interestingly, here, NCdMPC1 provides a slightly lower J_{sim} cost than NCdMPC. However, this could simply be due to the nature of the disturbance in this case. While space constraints do not permit it to be shown here, for more severe contingencies NCdMPC has a consistently lower value of J_{sim}, as would be expected. Typically, for various contingencies, the responses are quite similar in terms of damping, settling times, and minimisation of $\Psi_a(p)$, and so NCdMPC1 could suffice for use in reality where time constraints may not allow many NCdMPC iterations to be executed at each sample step.

7. CONCLUSIONS AND FUTURE WORK

In this paper a Non-Cooperative distributed MPC (NCdMPC) framework was proposed for Secondary Frequency

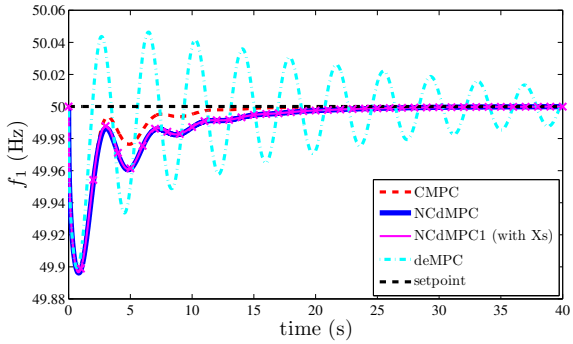

Fig. 2. Frequency response in area 1 for CMPC, NCdMPC, NCdMPC1, and deMPC cases.

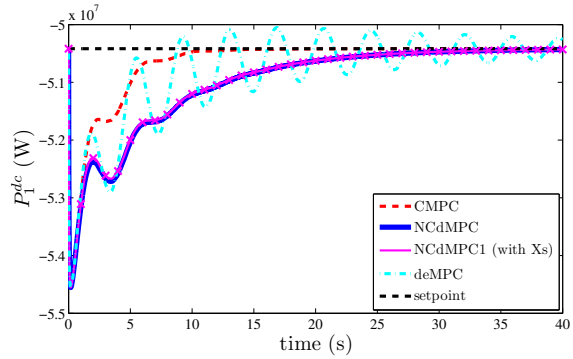

Fig. 3. HVDC power in area 1 for CMPC, NCdMPC, NCdMPC1, and deMPC cases.

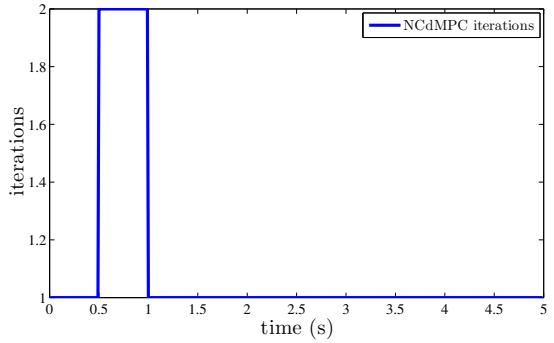

Fig. 4. Number of NCdMPC iterations needed over the course of the simulation (iterations remain at 1 after 5 s).

Control (SFC) of a Multi-Terminal HVDC (MTDC) system, under decentralised voltage based Primary Frequency Control, that avoids the need for a centralised coordinator. The effectiveness of the approach has been demonstrated with a simulation study. Future work will look at parallel implementations of NCdMPC, consider the robustness of this approach in terms of time delays and communication failures, and will investigate the use of additional constraints in the control formulation.

REFERENCES

Chaudhuri, N. and Chaudhuri, B. (2013). Adaptive Droop Control for Effective Power Sharing in Multi-Terminal DC (MTDC) Grids. *IEEE Transactions on Power Systems*, 28(1), 21–29.

Chaudhuri, N., Majumder, R., and Chaudhuri, B. (2013). System Frequency Support Through Multi-Terminal DC (MTDC) Grids. *IEEE Transactions on Power System*, 28(1), 347–356.

Christofides, P., Scattolini, R., Muñoz de la Peña, D., and Liu, J. (2013). Distributed model predictive control: A tutorial review and future research directions. *Computers & Chemical Engineering*, 51, 21–41.

Dai, J., Phulpin, Y., Sarlette, A., and Ernst, D. (2010). Impact of delays on a consensus-based primary frequency control scheme for AC systems connected by a multi-terminal HVDC grid. In *Proceedings of the iREP Symposium on Bulk Power System Dynamics and Control*, 1–9.

Dai, J., Phulpin, Y., Sarlette, A., and Ernst, D. (2012). Coordinated primary frequency control among non-synchronous systems connected by a multi-terminal high-voltage direct current grid. *IET Generation, Transmission Distribution*, 6(2), 99–108.

Dai, J. (2011). *Frequency control coordination among non-synchronous AC areas connected by a multi-terminal HVDC grid*. Ph.D. thesis, Supélec, France.

de Courreges d'Ustou, B. (2012). *Optimal Control Design For Multiterminal HVDC*. Ph.D. thesis, University of Pittsburgh.

Egea-Alvarez, A., Bianchi, F., Junyent-Ferre, A., Gross, G., and Gomis-Bellmunt, O. (2013). Voltage Control of Multiterminal VSC-HVDC Transmission Systems for Offshore Wind Power Plants: Design and Implementation in a Scaled Platform. *IEEE Transactions on Industrial Electronics*, 60(6), 2381–2391.

EWEA (2009). Pure power, wind energy targets for 2020 and 2030. Technical report, European Wind Energy Association.

Kundur, P. (1994). *Power System Stability and Control*. Mc-Graw Hill, New York.

Machowski, J., Kacejko, P., Nogal, L., and Wancerz, M. (2013). Power system stability enhancement by WAMS-based supplementary control of multi-terminal HVDC networks. *Control Engineering Practice*, 21(5), 583 – 592.

Maciejowski, J. (2002). *Predictive Control with Constraints*. Prentice Hall, Harlow, England.

Negenborn, R.R., De Schutter, B., and Hellendoorn, J. (2008). Multi-agent model predictive control for transportation networks: Serial versus parallel schemes. *Engineering Applications of Artificial Intelligence*, 21(3), 353–366.

Sarlette, A., Dai, J., Phulpin, Y., and Ernst, D. (2012). Cooperative frequency control with a multi-terminal high-voltage DC network. *Automatica*, 48(12), 3128 – 3134.

Silva, B., Moreira, C., Seca, L., Phulpin, Y., and Peas Lopes, J. (2012). Provision of Inertial and Primary Frequency Control Services Using Offshore Multiterminal HVDC Networks. *IEEE Transactions on Sustainable Energy*, 3(4), 800–808.

Van Hertem, D. and Ghandhari, M. (2010). Multi-terminal VSC HVDC for the European supergrid: Obstacles. *Renewable and sustainable energy reviews*, 14(9), 3156–3163.